

The New Permeability Pathways Induced by the Malaria Parasite in the Membrane of the Infected Erythrocyte: Comparison of Results Using Different Experimental Techniques

H. Ginsburg, W.D. Stein

Department of Biological Chemistry, The Institute of Life Sciences, The Hebrew University of Jerusalem, Jerusalem 91904, Israel

Received: 25 August 2003/Revised: 18 November 2003

Abstract. The membrane of erythrocytes infected with malaria parasites is highly permeable to a large variety of solutes, including anions, carbohydrates, amino acids, nucleosides, organic and inorganic cations and small peptides. The altered permeability is presumed to be due to the activation of endogenous dormant channels, the new permeability pathways. The latter have been studied by different techniques—isosmotic lysis and tracer fluxes—and recently by patch-clamping. Here we analyze all available published data and we show that there is generally a good agreement between the two first methods. From the fluxes we calculate the number of channels per cell using reasonable assumptions as to the radius of the channel, and assuming that penetration through the channel is by diffusion through a water-filled space. The number of channels so calculated is <10 for most solutes, but ~ 400 for anions and the nucleosides thymidine and adenosine. This latter number is not far from that calculated from patch-clamp experiments. However, the anion flux measured directly by tracer is an order of magnitude larger than expected from conductance measurements. We conclude that the new permeability pathways consist of two types of channels; one is present in small number, and is charge- and size-selective. The other type is about 100-fold more abundant and is anion-selective, but does not admit non-electrolytes other than perhaps nucleosides.

Key words: Malaria — *Plasmodium falciparum* — Infected erythrocyte — Membrane permeability — Anion channel — Comparative analysis

Introduction

During the intraerythrocytic phase of asexual development, a malaria parasite exhibits very intensive metabolic activity that allows it to replicate ~ 20 -fold within 48 hours. While the parasite develops, the permeability of the membrane of the infected red blood cell (RBC) increases gradually and significantly (Kirk, 2001). It is generally accepted that such an increased permeability is crucial in order to meet those of the parasite's metabolic demands that are not provided by the endogenous transport capacities of the uninfected RBC. Thus, the parasite must obtain purine bases (Upston & Gero, 1995) and pantothenic acid (Saliba et al., 1998) from the extracellular space and must release amino acids derived from the digestion of the cytosol (which consists predominantly of hemoglobin) of the infected cell (Krugliak et al., 2002) and release the lactic acid produced by the parasite, which has a 100-fold more intensive glycolytic activity than has the uninfected erythrocyte (Kanaani & Ginsburg, 1991; Cranmer et al., 1995; Elliott et al., 2001). The permeability increase has been assigned to new permeability pathways (NPPs), although their origin—from parasite-engendered channels or from the modification of host cell membrane proteins—is still debated.

Until recently NPPs were investigated by two techniques—measurement of the uptake of radio-labeled solutes and of the rate of hemolysis in isosmotic solutions of the investigated permeant (Kirk, 2001). These investigations revealed that the NPPs behave like an anion channel, admitting a large variety of unrelated solutes (carbohydrates, amino acids, short peptides and nucleosides) and also cations (K^+ , Na^+ and organic cations) to lesser, but considerable, degree. Compounds known to block other anion-selective channels also inhibit the NPPs, albeit at concentrations used such that the inhibitors

might be rather non-selective (Cabantchik & Greger 1992).

The investigation of the NPPs has recently been enhanced by the use of electrophysiological techniques, such as patch clamp. This has led to some advances but also some confusion. The first patch-clamp study identified an anion channel that was inhibited by the same compounds that inhibit NPPs, and it was concluded that the patch clamp had revealed properties of the NPPs (Desai et al., 2000). From whole-cell patch-clamp experiments, it was calculated that the channel is present at 1,000–2,000 copies per cell, that it was inwardly rectifying, and that it had a single-channel conductance of 3 pS. A subsequent study (Egee et al., 2002) identified only 200–300 channels/cell with a single-channel conductance of 12 pS. The anion selectivity of the channel was $I^- > Br^- > Cl^-$, similar to outwardly rectifying chloride channels and to volume-sensitive organic osmolyte and anion channels (Nilius & Droogmans, 2003). Concurrently, in a third study, an additional outwardly rectifying conductance has been identified (Huber et al., 2002). It was suggested that two anion-selective channel types, which act in parallel, must be induced by the parasite, the outwardly rectifying being responsible for the transport of electroneutral compounds. All these different channels are inhibited similarly by the same inhibitors of NPPs, casting additional doubts on the specificity of action of the inhibitors (Culliford et al., 2003).

The availability of radiotracer, hemolysis and electrophysiological data allows a deeper scrutiny of the characteristics of the NPPs. Here we will show (1) that for some permeants there is a substantial discrepancy between their rate of uptake (as measured by radiotracers) and the rate of hemolysis, and (2) that the number of channels calculated from uptake experiments differs by orders of magnitude from that derived from electrophysiological measurements. We confirm that there appear to be two classes of channels amongst the NPPs.

Methods

COMPARISON OF FLUX RATES TO $t_{1/2}$ OF ISOSMOTIC LYSIS

All studies that we review had been performed using RBC infected with the most lethal malaria parasite *Plasmodium falciparum*. All available data on transport rates of various radiolabeled solutes into these RBCs, and the half-time for lysis of infected cells in isosmotic solutions of the same solutes were collected from the literature. Since experiments were conducted at different temperatures (room temperature $\sim 22^\circ\text{C}$, or 37°C), all results were normalized to 22°C by dividing the data obtained at 37°C by 2.28 (a factor that is obtained from the enthalpy of activation A of sorbitol-induced lysis of 10 kcal/mol (Ginsburg et al., 1983; Kirk & Horner, 1995a) using the equation $D = D_0 e^{-A/RT}$ where D_0 is the

hypothetical diffusion coefficient at absolute zero, T is the absolute temperature, R is the gas constant (1.987 cal/mole)). Since flux data were obtained with different solute concentrations, they were all normalized to 1 mM and are expressed as $\mu\text{mole}/10^{13}$ cells/min/mm.

CALCULATION OF THE TIME TO LYSIS AND THE NUMBER OF NPPS PER CELL

The collected flux data were used to calculate the time for lysis (see Appendix A1) and the number of NPPs/cell (see Appendices A2 and A3).

Results

THE DISCREPANCY BETWEEN FLUX MEASUREMENTS AND HALF-TIME OF HEMOLYSIS

Table 1 presents data on flux measurements and $t_{1/2}$ for lysis for all the solutes for which we have found this pair of determinations. From the flux values we can compute an estimate of the time for lysis in order to compare this with the measured time. The calculations for two solutes are discussed in detail. Take first the case of glycine. The $t_{1/2}$ for isosmotic lysis at 22°C is 11.1 min. Flux (Ginsburg et al., 1986, Fig. 1) = $0.16 \mu\text{mol}/10^{10}$ cells/min (at 1 mM) at 37°C and the flux in $\mu\text{mole}/10^{13}$ cells/min/mm is calculated to be $0.16 \cdot 1000 = 160$, and 70.1 at 22°C . The time for lysis is calculated from the measured radiolabel flux and the assumption that enough solute has to enter the cells to swell it to the critical hemolytic volume (see Appendix A1). For glycine the calculated time for hemolysis is 13.32 minutes or 1.2 times the measured $t_{1/2}$.

Next, the case of thymidine. This solute is not incorporated by the parasite's metabolism and its uptake has been measured in the presence of nitrobenzylthioinosine, a specific inhibitor of the carrier-mediated nucleoside transport. The reported $t_{1/2}$ for isosmotic lysis at 37°C is 3.4 min and given the Q_{10} it is calculated to be 7.8 min at 22°C . The flux from Fig. 8 of Kirk et al. (1994) = $6200 \mu\text{mol}/10^{12}$ cells/hr (at 1 mM) (67% parasitemia) at 22°C and the flux in $\mu\text{mole}/10^{13}$ cells/min/mm is calculated to be $6200 \cdot 10/60/0.67 = 1542$. The calculated time to lysis is 0.61 minutes, 12.8 times faster than that measured.

Table 1 presents the data and results of these calculations for all the 20 solutes. For some solutes there is a fair agreement between the measured and calculated time for lysis (differing by a factor of less than ~ 2). For glutamine, *myo*-inositol and thymidine, the calculated time for lysis is substantially shorter than the measured $t_{1/2}$. For potassium and choline the results are ambiguous, depending on the source of data.

Table 1. Compilation of available data on radiolabel flux and $t_{1/2}$ of lysis in isosmotic media, and calculated time for lysis

Solute	$t_{1/2}$ for lysis 22°C min	Flux 22°C $\mu\text{mol}/10^{13}$ cells/min/mm	Calculated time for lysis (min) at 22°C	Measured $t_{1/2}$ /calculated time for lysis	Reference	
					Tracer	Lysis ⁶
Alanine	7.7	96.4	9.69	0.79	a	h
Glycine	11.1	70.1	13.32	0.83	a	h
Glutamine	100.0	61.3	15.23	6.57	a	h
Glutamate	25.0	35.9	26.04	0.96	b	h
Isoleucine	7.7	52.6	17.77	0.43	a	h
Sorbitol	9.6	79.9	11.69	0.82	c	i
Fructose ¹	47.9	73.6	12.69	2.62	a	Present
L-Glucose ²	33.3	30.7	30.46	1.57	d	e
Myo-inositol	350.0	10.9	85.28	4.10	a	h
Carnitine	49.5	46.9	19.92	2.48	e	e
Thymidine	7.8	1542.0	0.92	12.80	e	e
Choline-1 ³	75.0	9.9	94.75	0.79	e	e
Choline-2	102.0	16.4	56.85	1.79	f	f
Potassium ⁴	80.0	3.3	284.63	0.28	g	Present
Potassium	474.0	3.3	284.63	1.67	g	g
Sodium ⁴	450.0	2.7	519.98	0.87	g	Present
TMA ⁵	102.0	10.2	91.37	1.11	f	f
TEA	80.0	15.7	59.50	1.34	f	f
MTEA	56.7	23.4	39.97	1.42	f	f
PhTMA	4.1	153.3	6.09	0.67	f	f

¹The $t_{1/2}$ for fructose was determined in this investigation using the protocol of Ginsburg et al. (1985).

²The flux of L-glucose was calculated as shown in Appendix 4 from data of Kirk et al. (1996). For D-glucose, $t_{1/2}$ is obtained in the presence of 20 μM cytochalasin B to inhibit the endogenous glucose transporter.

³Since two different sets of values were reported in the literature, both were analyzed.

⁴The $t_{1/2}$ for lysis for potassium was obtained by suspending infected cells in a medium consisting of (in mM) 140 KCl, 2 NaCl, 10 NaSCN, 10 HEPES, pH 7.4, 22°C, and measuring extracellular hemoglobin at different time points. To obtain the $t_{1/2}$ for sodium, cells were suspended in a solution containing (in mM) 2 KCl, 137 NaCl, 10 NaSCN, 10 HEPES, pH 7.4. Lysis was measured up to 90 min and for sodium the extent of lysis was extrapolated to 50% assuming it is linear with time. The presence of 5 mM glucose had no effect on the lysis in the high-sodium medium and extended somewhat the $t_{1/2}$ for lysis in the high-potassium medium. The fluxes of potassium and sodium were taken from Staines et al. (2001). We take a value of 320 $\mu\text{mol}/10^{12}$ cells/h for rubidium, usually used as a surrogate for potassium (Fig. 3) at 5 mM (37°C) and convert to $\mu\text{mol}/10^{13}$ cells/min/mm to get 10.7. This value is multiplied by 0.7, the ratio of potassium to rubidium flux (Staines et al., 2001) to yield 7.49 $\mu\text{mol}/10^{13}$ cells/min/mm. For sodium (Fig. 5 of that article), the value is 3.7 $\text{mmol}/10^{12}$ cells/h at 150 mM. This converts to 4.1 $\mu\text{mol}/10^{13}$ cells/min/mm.

⁵TMA, tetramethylammonium; TEA, tetraethylammonium; MTEA, methyltriethylammonium; PhTMA, phenyltrimethylammonium.

⁶References used for flux and lysis data: a, Ginsburg et al. (1986); b, Kirk et al. (1999); c, Kirk & Horner (1995b); d, Kirk et al. (1996); e, Kirk et al. (1994); f, Staines et al. (2000); g, Staines et al. (2001); h, Ginsburg et al. (1985); i, Wagner et al. (2003).

DERIVATION OF THE NUMBER OF CHANNELS PER CELL FROM RADIOLABEL FLUXES

The flux, molecular volume and the diffusion coefficient of the various solutes are shown in Table 2. We first use these numbers to calculate the number of channels per cell (*see* Methods and Appendices). We next calculate the available area for diffusion, assuming a 5 Å radius channel. From these, we calculate the number of channels per cell corrected for the available area. For many of the non-electrolytes, this number is close to 4. We have used other values for the pore radius (from 4.5 to 6 Å) for the computation of the number of channels per cell. As expected, the computed number of channels decreases with increased postulated channel radius. It is 6.2 for a 4.5 Å channel and 2.6 for a 6 Å channel. A radius of 4.5 Å is already a major barrier for the entry of hydrated

sodium ions, and anything substantially smaller would exclude additional solutes (which *are* transported). In the Discussion we shall compare these numbers to those derived from the electrophysiological experiments.

AN ATTEMPT TO CHARACTERIZE THE DISCRIMINATORY BASIS OF THE CHANNEL

For a water-filled channel one might expect that the flux would be determined by the diffusion coefficient of the solute in water. The fluxes are plotted against the diffusion coefficient in Fig. 1A. No significant correlation is seen. Clearly, we are still missing some important determinants of channel selectivity. In what follows, all solutes were considered except for thymidine, adenosine, chloride, lactate and PhTMA, which deviate strongly from the others, and will be

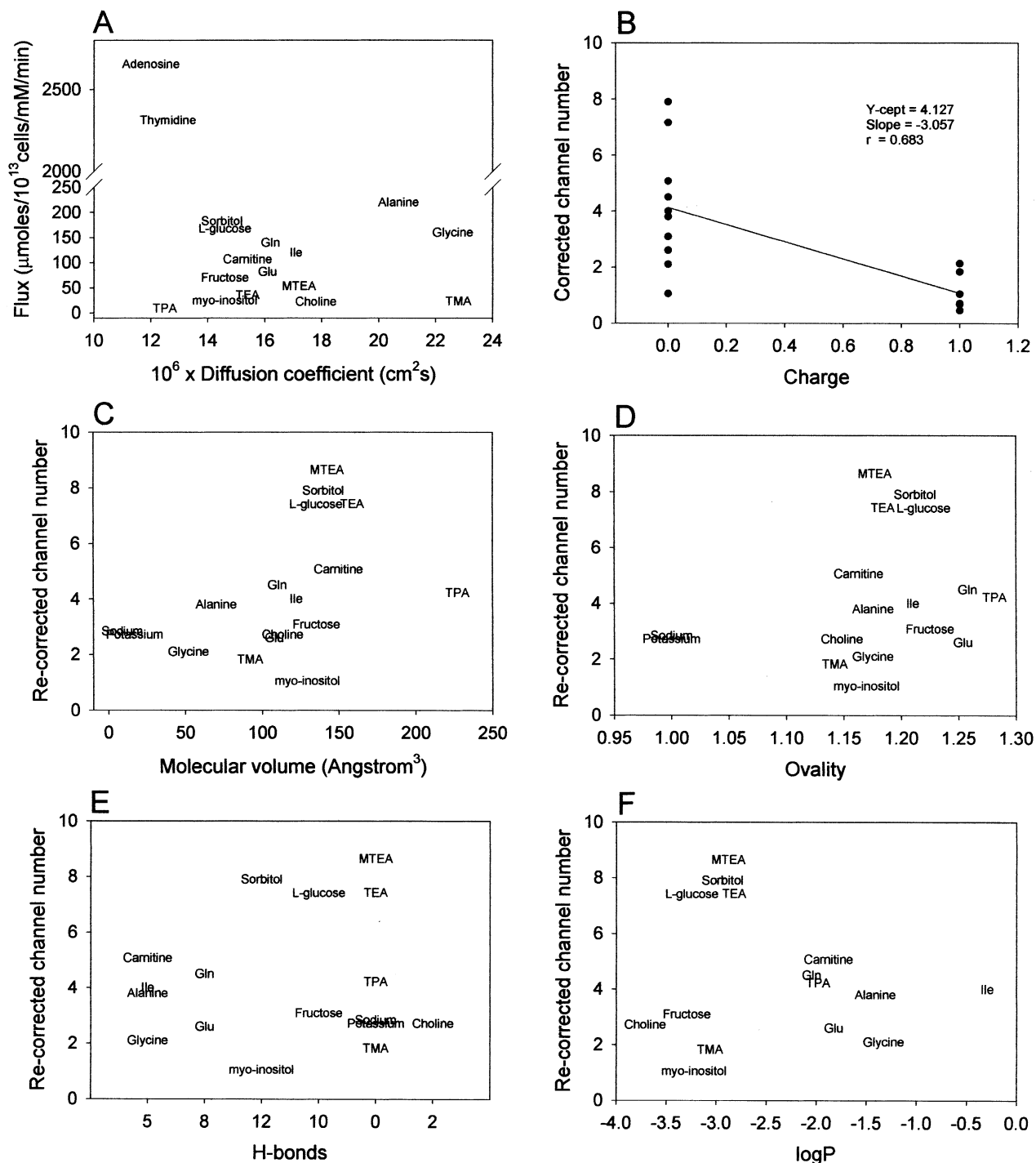


Fig. 1. Fluxes of the different solutes (at 37°C) were plotted against their diffusion coefficient (Table 2) in water (A) to find no correlation. (B) The numbers of channels per cell (Table 2) were plotted against the charge of the respective solute and linear regression was performed. The slope of the line was used to correct the calculated number of channels per cell as described in the text. The re-corrected channel numbers were plotted against the molecular volume (C), the ovality of the solute (D; see Appendix A3), the number of H-bonds that each solute can form (E) and the logarithm of octanol:water partition coefficient (F).

discussed separately. Since the solutes evaluated in this analysis also include cations, the effect of charge was investigated. The number of channels/cell (proportional to the flux) corrected for the available area

is plotted against the charge (Fig. 1B). The correlation found is significant at $p < 0.01$, $df = 13$. The slope of the linear regression line represents the average effect of charge, indicating that the channels are

negatively charged. For further analysis, the values of channels/cell corrected for available area for the cations have been multiplied by one plus the slope of the regression line, i.e., 4.06, to bring all solutes into a common ground ("re-corrected number of channels"). These re-corrected values are then plotted against the molecular volume (Fig. 1C), the ovality of the solute (Fig. 1D), the ability of the solute to form hydrogen bonds (Fig. 1E) and the logarithm of the octanol/water partition coefficient (Fig. 1F). No significant correlation could be found between the re-corrected number of channels/cell and any one of these parameters. Some solutes, such as sorbitol, L-glucose and MTEA remain stubbornly above from the rest, others such as TMA and *myo*-inositol fall below. Since values derived from data obtained by either of the two laboratories whose data are summarized in Table 2 are equally scattered around the average, the spread does not result from a consistent experimenter's bias.

The average number of channels/cell (\pm SD) for non-electrolytes (excluding thymidine and adenosine) is 4.14 ± 2.19 . For cations, the average is 1.08 ± 0.60 (making no allowance for any possible charge discrimination and without PhTMA) and for anions, 392.3 ± 37.0 .

Discussion

Recent electrophysiological investigations of the NPPs, which the intraerythrocytic malaria parasite induces in the membrane of its host cell, have reached the general conclusion that NPPs are endogenous channels that are activated by parasite action (Egee et al., 2002; Huber et al., 2002). However, different laboratories have reported different properties for the NPPs in terms of single-channel conductance, number of channels and rectification. Whatever may be the final resolution of these discrepancies, the biophysical parameters that were derived from the electrophysiological investigations must coincide with previously reported characterizations that were based on the direct measurement of uptake of radiolabeled solutes and on indirect assessments of the NPPs' permeability by iso-osmotic lysis. In the present analysis, all available data on radiolabel uptake and $t_{1/2}$ for lysis in isosmotic media were compiled and compared. The time for lysis of infected cells was calculated from the radiolabel flux and was found to agree with the measured $t_{1/2}$ for many solutes, including cations. The flux experiments were done at around 1 mM, while the isosmotic lysis experiments were done at 300 mM (150 mM for the cations). The good agreement found for many solutes between calculated time for lysis and $t_{1/2}$, irrespective of the possibility that they may be trapped by metabolism (all amino acids, choline) or not (L-glucose, sorbitol,

cations), suggests that a) the fluxes for these solutes do not saturate up to 300 mM, consistent with permeation through channels, and b) that the rate of metabolic trapping is probably much slower than the flux. However, for others, significant discrepancies were found, in that the calculated time for lysis is shorter (glutamine, *myo*-inositol and thymidine) than measured, while for isoleucine, it is longer. The calculation of the time to lysis assumes that the flux does not saturate. A measured $t_{1/2}$ significantly larger than calculated might suggest that for these solutes, the flux is saturating although for thymidine, the flux does not do so up to 10 mM (Kirk et al., 1994). There is evidently no common denominator for the solutes' presence in any group. The divergences might not stem from technical differences in the experimental techniques. Thus, although overlapping data exist only for very few solutes, when they are available, they are very similar among different laboratories. The radioactive flux of sorbitol measured by Ginsburg et al. (1986) and by Kirk and Horner (1995b) match very closely, and the $t_{1/2}$ for lysis in isosmotic solution of the same solute is very similar in two different reports (Ginsburg et al., 1985; Wagner et al., 2003). There is also a very good agreement for the flux of lactate (Kirk & Horner, 1995b; Kanaani & Ginsburg, 1991). On the other hand, there is almost a 2-fold discrepancy between choline fluxes and $t_{1/2}$ for lysis, coming from the same authors (*see* Table 1) and both sets of values were included in the analysis. Some of the discrepancies may arise from slight differences in stage of development of the parasites taken for the various measurements, as the evolution of the NPPs depends firmly on parasite development (Ginsburg et al., 1986) and particularly at the trophozoite stage that was generally used for these experiments (Staines et al., 2001). Beyond these caveats, the value of thymidine still stands out: The $t_{1/2}$ for lysis is ~ 13 times slower than expected from flux measurements. The reason for this discrepancy is not known but it is well established that some solutes have higher or lower affinities for protein surfaces (Courtenay et al., 2000). A high affinity for intra-erythrocytic hemoglobin may reduce the actual osmotic contribution of the solute and explain the longer than expected $t_{1/2}$ for lysis. It may be warranted to test other nucleosides (adenosine's insolubility prevented our attempt to do so in the isosmotic lysis experiments), to verify if this is a general phenomenon for this group of compounds.

Hemolysis studies are performed in low ionic strength media. It has been shown that suspending human red blood cells in low ionic strength medium induces a significant increase in membrane transport of glutamine, glutamate, lactate, histidine, taurine, glycine, serine, choline, potassium and carnitine but not sorbitol or sucrose (Culliford et al., 1995). The induced flux was inhibited by the same anion trans-

Table 2. Calculation of number of channels/cell from measured radiolabel fluxes and flux from the diffusion coefficient and the radius of solute and pore size

Solute	Flux at 37°C μmol/10 ¹³ cells/min/mm	MW	Molecular volume Å ³	D at 37°C cm ² /s	Channels/cell	Available area	Estimated channels/cell
Alanine	220	89.1	70.04	2.07E-05	0.90	0.2386	3.77
Glycine	160	75.07	52.09	2.26E-05	0.60	0.2879	2.09
Glutamine	140	146.15	109.98	1.62E-05	0.73	0.1644	4.49
Glutamate	81.87	147.13	107.87	1.61E-05	0.43	0.1675	2.57
Isoleucine	120	131.18	122.09	1.71E-05	0.60	0.1478	4.03
Sorbitol	182.3	182.17	139.97	1.45E-05	0.99	0.1265	7.86
L-Glucose ¹	168	180	135.26	1.46E-05	0.98	0.1365	7.16
Fructose ¹	70	180	135.19	1.46E-05	0.41	0.1319	3.09
Myo-inositol	25	180.16	129.32	1.46E-05	0.15	0.1387	1.05
Carnitine	107	161.2	149.82	1.54E-05	0.59	0.1162	5.07
Thymidine ²	3,520	242.23	183.08	1.26E-05	23.76	0.0873	272.38
Adenosine ²	4,041	267.25	189.67	1.20E-05	28.64	0.0824	347.68
Lactate ³	24,994	90.08	67.09	2.06E-05	102.86	0.2458	418.48
Chloride ³	54,087	35.45	29.28	3.29E-05	139.63	0.3814	366.15
Potassium ⁴	7.5	39.1	16.90	3.13E-05	0.02	0.0303	0.67
Sodium ⁴	4.1	22.99	8.92	4.08E-05	0.01	0.0121	0.70
Choline ⁵	22.5	121.18	113.33	1.78E-05	0.11	0.1596	0.67
TMA	23.3	74	92.17	2.28E-05	0.09	0.1931	0.45
TEA	35.8	161	158.88	1.54E-05	0.20	0.1075	1.83
TPA	9.0	247	227.26	1.25E-05	0.06	0.0589	1.04
MTEA	53.3	130	142.50	1.72E-05	0.26	0.1238	2.13
PhTMA	350	136	138.71	1.68E-05	1.77	0.1279	13.84

The number of channels/cell (column 6) was calculated with no correction for the available area, i.e., assuming that all the pore entry area is available for diffusion, while the estimated number of channels/cell (column 8) was corrected by the available area for diffusion.

¹The radius for glucose was calculated for glucopyranose and that for fructose, for fructofuranose. The flux of L-glucose was derived as shown in Appendix A4.

²The fluxes for thymidine and adenosine were taken from Kirk et al. (1994).

³The fluxes of lactate and chloride were derived as shown in the Appendix.

⁴The radii for potassium and sodium were calculated for the hydrated cation—2 molecules of water.

⁵The fluxes of choline and the organic cations were taken from Staines et al. (2000).

port inhibitors that inhibit NPPs. Of the molecules on this list, glutamate, glycine and choline do not deviate appreciably if $t_{1/2}$ and fluxes are compared. Sorbitol, which is not on the list of deviants, does not have its permeability increased by low ionic strength. Thus, the low ionic strength effect may not be important in accounting for the $t_{1/2}$ -flux deviations.

The merits and possible shortcomings of the isosmotic lysis technique have been discussed critically in a recent review on the NPPs (Kirk, 2001), where the method is commended because it requires small amounts of infected cells, it does not necessitate the separation of infected from uninfected cells and the use of expensive radioisotopes. Several significant limitations were also mentioned and the present analysis bears on their detailed evaluation.

Kirk notes that “The technique uses high concentrations of the investigated solute. A potential hazard of the technique is the exposure of the cells to non-physiological conditions that may affect the function of the NPPs and fall in the range of saturation.” This is hypothetically true, but we found that for most solutes there is a fair agreement between

predicted and measured $t_{1/2}$ of lysis. This concurrence indicates that the operation of the pathways is not considerably modified by the environment, if at all, and that it is not saturated. Saturation would produce a $t_{1/2}$ for lysis that is longer than calculated from flux at low solute concentration. Hence, the ratio of measured to calculated, using flux data, should be > 1 . Inspection of Table 1 shows that within a factor of ~ 2 , the number of cases with > 1 is essentially equal to that with ratios < 1 . Given the possible experimental errors, it seems safe to conclude that for most solutes there is no saturation. The take-home message is that measurement of the permeability of solutes (provided they can be dissolved to the necessary concentrations) by the isosmotic lysis technique is both accurate, informative and economical.

Next, Kirk notes that “the rate of hemolysis can in principle be altered by binding or metabolization of the penetrating solute.” This possibility must indeed be considered, but it is very unlikely that sufficient metabolic trapping or metabolization can occur within the short times of the lysis experiment to affect the total intracellular concentration of solute.

Also, enzymes have K_m s that are in the mM range or below, and they will become very quickly saturated when exposed to high concentrations of the penetrating solute. Thus, their maximal activity will probably never match the high rate of solute uptake, so that metabolism will probably involve a tiny fraction of the penetrating solute and cannot be quantitatively important to the buildup or reduction of osmotic pressure.

The radiolabel flux values were used to derive the number of channels per cell (Table 2). For all non-electrolytes and cations, the calculated number of channels is 4.14 and 1.07, respectively. A similar small number of channels/cell was previously proposed using a similar analytical approach (Ginsburg et al., 1986). These low numbers are at least two orders of magnitude smaller than that calculated from electrophysiological studies: from 200–300 (Egee et al., 2002) to 1,000–2,000 (Desai et al., 2000).

The fluxes of thymidine, adenosine, chloride and lactate, which have been left out of the discussion up to now, need to be further considered. It will be seen from Table 2 that the calculated number of channels corrected for available area for these 4 solutes is similar to the number reported in the electrophysiological data and is nearly 100 times the number of channels calculated for the non-electrolytes. It would appear that the anions and the nucleosides enter by a channel or channels that is different from that of the non-electrolytes and cations. It seems therefore that there are at least two types of channels, one probably mediating the fluxes of non-electrolytes and cations (discriminating between these two groups of solutes on the basis of charge, preferentially slowing cation diffusion four-fold), while the other is dedicated to the translocation of anions. The first, charge-discriminating, type should be able to translocate anions about 4-fold the rate of transport of non-electrolytes. Were this to be the case, these channels will provide about 4% of the total anion flux and would probably not be seen in patch-clamp experiments.

It is still necessary to explain the high fluxes of the nucleosides thymidine and adenosine. As the number of channels calculated for these nucleosides (310) is about 4/5 that retrieved from the fluxes of lactate and chloride (392), could their transport be mediated by the exclusively anion channel? Their molecular volumes imply that other non-electrolytes should also be able to go through these channels, but then the number of channels for non-electrolytes should be 310 on the average compared to the calculated 4.14. Perhaps the predominant anion channels are unusually permeable to nucleosides, but not to other non-electrolytes.

We now calculate the flux of chloride from patch-clamp experiments and compare the result to the measured radiolabel flux. We take from Egee et

al. (2002) a total conductance of 5,300 pS/cell for infected RBC. The current through the pores of a single cell at 10 mV membrane potential will be $53 \cdot 10^{-12}$ Coulombs/s. Dividing by Faraday (Coulombs/equivalent), we get $5.49 \cdot 10^{-16}$ moles/cell/s. We now convert to 10^{13} cells/min and get 329 mmoles/ 10^{13} cells/min. We now divide this by 175 mM (the chloride concentration in the pipette and the bathing solutions) and get, as a measure of the chloride flux, 1.88 mmoles/ 10^{13} cells/min/mM. As another estimate, we can calculate similarly from Huber et al. (2002) who identified two types of channels: one inwardly rectifying with a conductance of 7,000 pS and one outwardly rectifying with a conductance of 18,000 pS. With a bathing solution containing 145 mM Cl^- , this translates to 3.0 and 7.72 mmoles/ 10^{13} cells/min/mM, respectively. These values should be compared to the substantially higher value of 54.1 mmoles/ 10^{13} cells/min/mM as measured by radiolabel (Table 2). It should be noticed that the chloride flux was determined in the presence of 4,4'-diisothiocyanostilbene-2,2'-disulfonic acid (DIDS), an inhibitor of the anion exchanger. In the patch-clamp experiments DIDS either inhibits (Huber et al., 2002) or does not affect whole-cell conductance (Egee et al., 2002). Desai et al. (2000) reported a whole-cell conductance of 150 nS/M equal to 150 pS/mM/cell (no effect of DIDS has been recorded). This is ~ 5 -fold larger than measured by Egee et al. (2002), giving 9.4 mmoles/ 10^{13} cells/min/mM, still leaving a substantial discrepancy between the electrophysiological data and directly measured chloride uptake. We note, however, that the number of channels calculated for anions in the present analysis is not very different from that found in the patch-clamp analysis. It could be that both types of studies are looking at the same type of channels. Why then are the flux data so much higher than can be calculated from the conductances? Flux determined by radiolabeled Cl^- measures both electrically silent and non-silent movements of the anion, and this may be a possible source for the discrepancy. It is possible that the conductances measure the movement of net charge whereas the fluxes are measuring predominantly anion exchange, but both go through the same channel. Is the charge movement a tunneling through an anion exchanger? (Frohlich, 1988.)

Durantón et al. (2003) have recently documented a novel slightly cation-selective channel that is revealed when chloride is essentially absent. Since the whole-cell conductance of this pathway is 2,000 pS, repeating the calculations shown above for the Cl^- conductance, the expected Na^+ flux is 124 mmol/ 10^{13} cells/min. Since the bathing solution contains 144 mM Na^+ , the calculated flux is 0.86 mmol/ 10^{13} cells/min/mM, about 210-fold larger than measured with radiotracer (Table 2). Is this an artifact of removal of Cl^- .

In conclusion, the data on the flux, hemolysis and conductances cannot be counted for on the basis of a single species of channel. However, the data can be largely understood in terms of permeation through two types of channels. One channel is present in a small number of copies per cell, about 4, it discriminates against cations by a factor of 4, but does not discriminate in terms of the ovality, the H-bonding capacity or the partition coefficient of the solute. The second type of channel is present in hundreds of copies per cell, and allows the movement of anions and nucleosides. It may allow anions to permeate in both the exchange and in the net modes, the former predominating. It may be possible in the future to find agents that block selectively these two channel types. Presently available inhibitors do not.

Appendix A1

CALCULATION OF THE TIME TO LYSIS

The lysis of IRBC in iso-osmotic media (300 mM of the penetrating solute) depends on the rate of uptake of the permeating solute. In order to compare the measured $t_{1/2}$ of lysis to the measured flux, we calculated from the measured radiolabel flux the time needed to reach an intracellular concentration of 200 mM of the penetrating solute. Such an increase in intracellular osmotic concentration should swell the cell to its critical hemolytic volume of $\sim 145 \mu^3$ and cause lysis. To calculate the time t for lysis, we derive from equation A3.4 of Stein (1990; pp. 314) the following:

$$\ln \frac{S_{\text{out}}}{S_{\text{out}} - \frac{2}{3} S_{\text{out}}} = \frac{P \cdot A \cdot t}{V}$$

where P is the permeability, A is the surface area and V is the volume. The left-hand side of the equation equals $\ln 3 = 1.0986$.

$$\text{flux} = P \cdot A \cdot \Delta C = P \cdot N \cdot \bar{A} \cdot \Delta C$$

$$\begin{aligned} \text{flux} &= \frac{1.0986 \cdot 85 \cdot 10^{-12} \text{cm}^3 \cdot 10^{13} \text{cells} \cdot \mu\text{moles}}{t_{2/3} \text{ min}} \\ &= \frac{933.8 \mu\text{moles}}{t_{2/3} \text{ min} \cdot \text{mM} \cdot 10^{13} \text{cells}} \end{aligned}$$

where \bar{A} is the surface area of one cell, N is the number of cells. Hence, to get $t_{2/3}$ we divide 933.8 by the flux given in $\mu\text{mole}/10^{13} \text{ cells}/\text{min}/\text{mM}$.

Appendix A2

CALCULATION OF THE NUMBER OF NPPs PER CELL

The following equation has been used to calculate the number of channels per cell.

$$\begin{aligned} n &= \frac{\text{flux} \cdot \lambda}{D \cdot A \cdot \Delta C} \\ &= \frac{\text{flux} \cdot \mu\text{mole} \cdot 10^3 \text{cm}^3 \cdot 40 \cdot 10^{-8} \text{cm}^2 \cdot \text{s} \cdot \text{mmol}}{10^{13} \text{cells} \cdot \text{mmol} \cdot 60 \cdot \text{s} \cdot D \cdot \text{cm}^2 \cdot 78.54 \text{cm}^2 \cdot 10^3 \mu\text{mol}} \end{aligned}$$

Flux is inserted as $\mu\text{mo}/10^{13} \text{ cells}/\text{mM}/\text{min}$. The value of λ (membrane thickness) is taken as $40 \cdot 10^{-8} \text{cm}$; ΔC (concentration

gradient) = 1 mM, because all fluxes were normalized to 1 mM; D (diffusion coefficient) is in $\text{cm}^2 \cdot \text{s}^{-1}$; A is the cross section of a channel radius of $5 \cdot 10^{-8} \text{cm}$ (Kirk et al., 1999), hence the cross section is $\pi \cdot r^2 = 78.54 \cdot 10^{-16} \text{cm}^2$.

Finally, the result is divided by the calculated available area for diffusion, since a solute will pass through the channel only if it does not hit the channel wall. The available area is approximately given by $(1-r/R)^2$ where r is the solute radius (calculated from the volume, see Appendix A3) and R is the channel radius (5 Å). See Stein, 1990, pp 90–91.

Appendix A3

CALCULATION OF THE SIZE OF SOLUTES AND THEIR DIFFUSION COEFFICIENTS

The volume of the various solutes has been calculated using ChemOffice2001© to draw the structure of the solute. This structure is then used by the CSChem3D Ultra program to minimize the energy of the solute structure to obtain the Connolly-solvent-excluded volume, which is very close to the classical Bondi volume (Connolly, 1993). The Connolly solvent-excluded volume is the volume contained within the contact molecular surface created when a spherical probe sphere (representing the solvent; the radius of the solvent used was 1.4 Å) is rolled over the molecular model. From this value, the radius and subsequently the cross-section have been calculated. In these calculations we have assumed that the molecules are ideal spheres. This will certainly not always be the case. Particularly, sorbitol is definitely closer to a cylinder. Thus, the ovality of each molecule—the ratio of the surface area to the minimum surface area (of a sphere having a volume equal to the solvent-excluded volume of the molecule)—has also been estimated. This program was also used to calculate the octanol-to-water partition coefficients of the non-electrolytes, while those for organic cations were taken from Staines et al., 2000. The diffusion coefficient for most smaller aqueous species, including organics, is similar, differing by, at most, a factor of two from the self-diffusion coefficient of water, which is $2.4 \times 10^{-5} \text{cm}^2/\text{s}$ at 25°C. Since it has been shown that $D \cdot M^{1/2} = \text{constant}$ up to a molecular weight of some 100 (Stein, 1967), the following equation has been used to calculate D for all solutes used in this analysis.

$$D_{\text{solute}} = \sqrt{\frac{\text{MW}_{\text{water}}}{\text{MW}_{\text{solute}}}} D_{\text{water}}$$

All calculated values were multiplied by 1.923 in order to normalize them to 37°C. The number of hydrogen bonds per molecule was calculated from Table 3.2 of Stein, 1967.

Appendix A4

CALCULATION OF L-GLUCOSE FLUX FROM $t_{1/2}$ OF TRACER EQUILIBRATION

$$\begin{aligned} \text{flux} &= P \cdot A \cdot \Delta C \\ &= P \cdot N \cdot \bar{A} \cdot \Delta C \\ t_{1/2} &= \frac{0.693 \cdot V}{P \cdot A} \end{aligned}$$

$$\begin{aligned} \text{flux} &= \frac{0.693 \cdot V \cdot N \cdot \Delta C}{t_{1/2}} \\ &= \frac{0.693 \cdot 85 \cdot 10^{-12} \text{ cm}^3 \cdot 10^{13} \text{ cells} \cdot \mu\text{moles}}{t_{1/2} \text{ min}} \\ &= \frac{589 \mu\text{mol}}{t_{1/2} \text{ min} \cdot \text{mm} \cdot 10^{13} \text{ cells}} \end{aligned}$$

From Kirk et al. (1996) Fig. 2c for L-glucose at 37°C, we calculate $t_{1/2}$ with and without furosemide to be 84 and 3.33 min. We subtract the reciprocals of these values and take the reciprocal of the difference = 3.47 min. The flux = $589/3.47 = 168 \mu\text{mol}/10^{13} \text{ cells}/\text{min}/\text{mm}$.

CALCULATION OF LACTATE AND CHLORIDE FLUXES

The data from Kirk et al. (1994) were used for this calculation. $[\text{lactate}]_0 = 1 \text{ mM}$; $T = 22^\circ\text{C}$. Parasitemia = 81%. The data presented in Fig. 9A of that publication were digitized and analyzed with Sigmaplot® to fit a the cellular concentration (C_i) change with time to a double exponential $C_i = a \cdot (1 - \exp^{-b \cdot t}) + c \cdot (1 - \exp^{-d \cdot t})$, which was found to fit best the data (correlation coefficient = 0.999). The parameters retrieved were: $a = 39.2 \pm 4.3$; $b = 22.6 \pm 4.1$; $c = 52.1 \pm 3.8$ and $d = 2.0 \pm 0.32$. The initial rate (in $\mu\text{mol}/10^{12} \text{ cells}/\text{min}/\text{mm}$) given by the product of $a \cdot b$ is 886.8; $c \cdot d = 104.2$. The second exponential may represent either the parasite compartment or a second subpopulation of cells. The values of the first exponential were used to calculate the initial rate. Hence the flux at 22°C equals $8,868 \mu\text{mol}/10^{13} \text{ cells}/\text{min}/\text{mm}$, and corrected for 100% parasitemia it is 10,948, and at 37°C it is $24,994 \mu\text{mol}/10^{13} \text{ cells}/\text{min}/\text{mm}$. For the fluxes of chloride, we take the ratio between chloride and lactate fluxes displayed in Fig. 10 of the same publication, which is 2.164, and multiply the calculated flux of lactate by this ratio. Hence, the flux of chloride at 37°C = $54,087 \mu\text{mol}/10^{13} \text{ cells}/\text{min}/\text{mm}$.

We thank Drs. V.L. Lew, S.L.Y. Thomas, S.M. Huber, H.M. Staines and K. Kirk for critical reading of an earlier version of this report and for their valuable suggestions. Thanks are also extended to M. Krugliak for performing the experiments reported herein.

References

Cabantchik, Z.I., Greger, R. 1992. Chemical probes for anion transporters of mammalian cell membranes. *Am. J. Physiol.* **262**:C803–C827

Connolly, M.L. 1993. The molecular surface package. *J. Mol. Graph.* **11**:139–141

Courtenay, E.S., Capp, M.W., Anderson, C.F., Record, M.T., Jr. 2000. Vapor pressure osmometry studies of osmolyte-protein interactions: implications for the action of osmoprotectants in vivo and for the interpretation of “osmotic stress” experiments in vitro. *Biochemistry* **39**:4455–4471

Cranmer, S.L., Conant, A.R., Gutteridge, W.E., Halestrap, A.P. 1995. Characterization of the enhanced transport of L- and D-lactate into human red blood cells infected with *Plasmodium falciparum* suggests the presence of a novel saturable lactate proton cotransporter. *J. Biol. Chem.* **270**:15045–15052

Culliford, S., Ellory, C., Lang, H.J., Englert, H., Staines, H., Wilkins, R. 2003. Specificity of classical and putative Cl⁻ transport inhibitors on membrane transport pathways in human erythrocytes. *Cell. Physiol. Biochem.* **13**:181–188

Culliford, S.J., Bernhardt, I., Ellory, J.C. 1995. Activation of a novel organic solute transporter in mammalian red blood cells. *J. Physiol.* **489**:755–765

Desai, S.A., Bezrukov, S.M., Zimmerberg, J. 2000. A voltage-dependent channel involved in nutrient uptake by red blood cells infected with the malaria parasite. *Nature* **406**:1001–1005

Duranton, C., Huber, S., Tanneur, V., Lang, K., Brand, V., Sandu, C., Lang, F. 2003. Electrophysiological properties of the *Plasmodium falciparum*-induced cation conductance of human erythrocytes. *Cell. Physiol. Biochem.* **13**:189–198

Egee, S., Lapaix, F., Decherf, G., Staines, H.M., Ellory, J.C., Doerig, C., Thomas, S.L. 2002. A stretch-activated anion channel is up-regulated by the malaria parasite *Plasmodium falciparum*. *J. Physiol.* **542**:795–801

Elliott, J.L., Saliba, K.J., Kirk, K. 2001. Transport of lactate and pyruvate in the intraerythrocytic malaria parasite, *Plasmodium falciparum*. *Biochem. J.* **355**:733–739

Frohlich, O. 1988. The “tunneling” mode of biological carrier-mediated transport. *J. Membrane Biol.* **101**:189–198

Ginsburg, H., Krugliak, M., Eidelman, O., Cabantchik, Z. 1983. New permeability pathways induced in membranes of *Plasmodium falciparum* infected erythrocytes. *Mol. Biochem. Parasitol.* **8**:177–190

Ginsburg, H., Kutner, S., Krugliak, M., Cabantchik, Z. 1985. Characterization of permeation pathways appearing in the host membrane of *Plasmodium falciparum* infected red blood cells. *Mol. Biochem. Parasitol.* **14**:313–322

Ginsburg, H., Kutner, S., Zangvill, M., Cabantchik, Z.I. 1986. Selectivity properties of pores induced in host erythrocyte membranes by *Plasmodium falciparum*: Effect of parasite maturation. *Biochim. Biophys. Acta.* **861**:194–196

Huber, S.M., Uhlemann, A.C., Gamper, N.L., Duranton, C., Kremsner, P.G., Lang, F. 2002. *Plasmodium falciparum* activates endogenous Cl⁻ channels of human erythrocytes by membrane oxidation. *EMBO J.* **21**:22–30

Kanaani, J., Ginsburg, H. 1991. Transport of lactate in *Plasmodium falciparum* infected human erythrocytes. *J. Cell. Physiol.* **149**:469–476

Kirk, K. 2001. Membrane transport in the malaria-infected erythrocyte. *Physiol. Rev.* **81**:495–537

Kirk, K., Horner, H.A. 1995a. In search of a selective inhibitor of the induced transport of small solutes in *Plasmodium falciparum*-infected erythrocytes: Effects of arylaminobenzoates. *Biochem. J.* **311**:761–768

Kirk, K., Horner, H.A. 1995b. Novel anion dependence of induced cation transport in malaria-infected erythrocytes. *J. Biol. Chem.* **270**:24270–24275

Kirk, K., Horner, H.A., Elford, B.C., Ellory, J.C., Newbold, C.I. 1994. Transport of diverse substrates into malaria-infected erythrocytes via a pathway showing functional characteristics of a chloride channel. *J. Biol. Chem.* **269**:3339–3347

Kirk, K., Horner, H.A., Kirk, J. 1996. Glucose uptake in *Plasmodium falciparum*-infected erythrocytes is an equilibrative not an active process. *Mol. Biochem. Parasitol.* **82**:195–205

Kirk, K., Staines, H.M., Martin, R.E., Saliba, K.J. 1999. Transport properties of the host cell membrane. In: Transport and Trafficking in the Malaria-Infected Erythrocyte, pp. 55–66. John-Wiley & Sons, Chichester.

Krugliak, M., Zhang, J., Ginsburg, H. 2002. Intraerythrocytic *Plasmodium falciparum* utilizes only a fraction of the amino acids derived from the digestion of host cell cytosol for the biosynthesis of its proteins. *Mol. Biochem. Parasitol.* **119**:249–256

Nilius, B., Droogmans, G. 2003. Amazing chloride channels: an overview. *Acta. Physiol. Scand.* **177**:119–147

- Saliba, K.J., Horner, H.A., Kirk, K. 1998. Transport and metabolism of the essential vitamin pantothenic acid in human erythrocytes infected with the malaria parasite. *Plasmodium falciparum*. *J. Biol. Chem.* **273**:10190–10195
- Staines, H.M., Ellory, J.C., Kirk, K. 2001. Perturbation of the pump-leak balance for Na⁺ and K⁺ in malaria-infected erythrocytes. *Am. J. Physiol. Cell. Physiol.* **280**:C1576–C1587
- Staines, H.M., Rae, C., Kirk, K. 2000. Increased permeability of the malaria-infected erythrocyte to organic cations. *Biochim. Biophys. Acta. Biomembranes.* **1463**:88–98
- Stein, W.D. 1967. *The Movement of Molecules Across Cell Membranes*. Academic Press, New York.
- Stein, W.D. 1990. *Channels, Carriers, and Pumps: An Introduction to Membrane Transport*. Academic Press, San Diego.
- Upston, J.M., Gero, A.M. 1995. Parasite-induced permeation of nucleosides in *Plasmodium falciparum* malaria. *Biochim. Biophys. Acta-Biomembranes.* **1236**:249–258
- Wagner, M.A., Andemariam, B., Desai, S.A. 2003. A two-compartment model of osmotic lysis in *Plasmodium falciparum*-infected erythrocytes. *Biophys. J.* **84**:116–123